PID Controller Design for Specified Performance

Štefan Bucz and Alena Kozáková
Institute of Control and Industrial Informatics,
Faculty of Electrical Engineering and Information Technology,
Slovak University of Technology, Bratislava
Slovak Republic

1. Introduction

„How can proper controller adjustments be quickly determined on any control application?" The question posed by authors of the first published PID tuning method J.G.Ziegler and N.B.Nichols in 1942 is still topical and challenging for control engineering community. The reason is clear: just every fifth controller implemented is tuned properly but in fact:

- 30% of improper performance is due to inadequate selection of controller design method,
- 30% of improper performance is due to neglected nonlinearities in the control loop,
- 20% of improper closed-loop dynamics is due to poorly selected sampling period.

Although there are 408 various sources of PID controller tuning methods (O´Dwyer, 2006), 30% of controllers permanently operate in manual mode and 25% use factory-tuning without any up-date with respect to the given plant (Yu, 2006). Hence, there is natural need for effective PID controller design algorithms enabling not only to modify the controlled variable but also achieve specified performance (Kozáková et al., 2010), (Osuský et al., 2010). The chapter provides a survey of 51 existing practice-oriented methods of PID controller design for specified performance. Various options for design strategy and controller structure selection are presented along with PID controller design objectives and performance measures. Industrial controllers from ABB, Allen&Bradley, Yokogawa, Fischer-Rosemont commonly implement built-in model-free design techniques applicable for various types of plants; these methods are based on minimum information about the plant obtained by the well-known relay experiment. Model-based PID controller tuning techniques acquire plant parameters from a step-test; useful tuning formulae are provided for commonly used system models (FOPDT – first-order plus dead time, IPDT – integrator plus dead time, FOLIPDT – first-order lag and integrator plus dead time and SOPDT – second-order plus dead time). Optimization-based PID tuning approaches, tuning methods for unstable plants, and design techniques based on a tuning parameter to continuously modify closed-loop performance are investigated. Finally, a novel advanced design technique based on closed-loop step response shaping is presented and discussed on illustrative examples.

2. PID controller design for performance

Time response of the controlled variable y(t) is modifiable by tuning proportional gain K, and integrating and derivative time constants T_i and T_d, respectively; the objective is to achieve a zero steady-state control error e(t) irrespective if caused by changes in the reference w(t) or the disturbance d(t). This section presents practice-oriented PID controller design methods based on various perfomance criteria. Consider the control-loop in Fig. 1 with control action u(t) generated by a PID controller (switch SW in position "1").

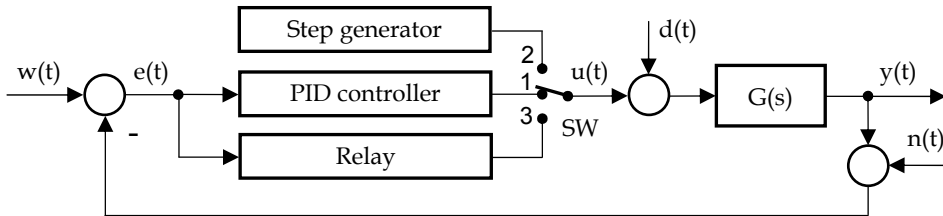
Fig. 1. Feedback control-loop with load disturbance d(t) and measurement noise n(t)

A controller design is a two-step procedure consisting of controller structure selection (P, PI, PD or PID) followed by tuning coefficients of the selected controller type.

2.1 Selection of PID controller structure
Appropriate structure of the controller $G_R(s)$ is usually selected with respect to zero steady-state error condition (e(∞)=0), type, and parameters of the controlled plant.

2.1.1 Controller structure selection based on zero steady-state error condition
Consider the feedback control loop in Fig. 1 where G(s) is the plant transfer function. According to the Final Value Theorem, the steady-state error

$$e(\infty) = \lim_{s \to 0} sE(s) = \lim_{s \to 0} s \frac{1}{1+L(s)} W(s) = q! w_q \lim_{s \to 0} \frac{s^{\nu - q}}{s^{\nu} + K_L} \tag{1}$$

is zero if in the open-loop L(s)=G(s)$G_R(s)$, the integrator degree $\nu_L = \nu_S + \nu_R$ is greater than the degree q of the reference signal w(t)=$w_q t^q$, i.e.

$$\nu_L > q \tag{2}$$

where ν_S and ν_R are integrator degrees of the plant and controller, respectively, K_L is open-loop gain and w_q is a positive constant (Harsányi et al., 1998).

2.1.2 Principles of controller structure selection based on the plant type
Industrial process variables (e.g. position, speed, current, temperature, pressure, humidity, level etc.) are commonly controlled using PI controllers. In practice, the derivative part is usually switched off due to measurement noise. For pressure and level control in gas tanks, using P controller is sufficient (Bakošová & Fikar, 2008). However, adding derivative part improves closed-loop stability and steepens the step response rise (Baláté, 2004).

2.1.3 PID controller structure selection based on plant parametres

Consider the FOPDT (j=1) and FOLIPDT (j=3) plant models given as $G_{FOPDT}=K_1 e^{-D_1 s}/[T_1 s+1]$ and $G_{FOLIPDT}=K_3 e^{-D_3 s}/\{s[T_3 s+1]\}$ with following parameters

$$\tau_1 = \frac{D_1}{T_1}\,; \quad \rho_1 = K_1 K_c\,; \quad \tau_3 = \frac{D_3}{T_3}\,; \quad \rho_3 = \frac{\lim\limits_{s \to 0} sG(s)}{\omega_c |G(j\omega_c)|} = \frac{T_c K_3 K_c}{2\pi}\,; \quad \tau_3 = \frac{\frac{2}{\pi} + arctg\sqrt{\rho_3^2 - 1}}{\sqrt{\rho_3^2 - 1}} \quad (3)$$

where K_c and ω_c are critical gain and frequency of the plant, respectively. Normed time delay τ_j and parameter ρ_j can be used to select appropriate PID control strategy. According to Tab. 1 (Xue et al., 2007), the derivative part is not used in presence of intense noise and a PID controller is not appropriate for plants with large time delays.

Ranges for τ and ρ	No precise control necessary	Precise control needed		
		High noise	Low saturation	Low measurement noise
$\tau_1 > 1$; $\rho_1 < 1,5$	I	I+B+C	PI+B+C	PI+B+C
$0,6 < \tau_1 < 1$; $1,5 < \rho_1 < 2,25$	I or PI	I+A	PI+A	(PI or PID)+A+C
$0,15 < \tau_1 < 0,6$; $2,25 < \rho_1 < 15$	PI	PI	PI or PID	PID
$\tau_1 < 0,15$; $\rho_1 > 15$ or $\tau_3 > 0,3$; $\rho_3 < 2$	P or PI	PI	PI or PID	PI or PID
$\tau_3 < 0,3$; $\rho_3 > 2$	PD+E	F	PD+E	PD+E

Table 1. Controller structure selection with respect to plant model parameters:
A: forward compensation suggested, B: forward compensation necessary, C: dead-time compensation suggested, D: dead-time compensation necessary, E: set-point weighing necessary, F: pole-placement

2.2 PID controller design objectives

Consider the following most frequently used PID controller types: ideal PID (4a), real interaction PID with derivative filtering (4b) and ideal PID in series with a first order filter (4c)

$$G_R(s) = K\left(1 + \frac{1}{T_i s} + T_d s\right)\,; \quad G_R(s) = K\left(1 + \frac{1}{T_i s} + \frac{T_d s}{1 + \frac{T_d}{N}s}\right)\,; \quad G_R(s) = K\left(1 + \frac{1}{T_i s} + T_d s\right)\left(\frac{1}{T_f s + 1}\right) (4)$$

In practical cases $N \in \langle 8;16 \rangle$ (Visoli, 2006). The PID controller design objectives are:
1.   tracking of setpoint or reference variable w(t) by y(t),
2.   rejection of disturbance d(t) and noise n(t) influence on the controlled variable y(t).
The first objective called also „servo-tuning" is frequent in motion systems (e.g. tracking required speed); techniques to guarantee the second objective are called „regulator-tuning".

2.3 Performance measures in the time domain

Performance measures indicating satisfactory quality of setpoint tracking (Fig. 2a) and disturbance rejection (Fig. 2b) are small maximum overshoot and small decay ratio, respectively, given as

$$\eta_{\max} = 100\frac{|y_{\max} - y(\infty)|}{y(\infty)} \ [\%]; \ \ \delta_{DR} = \frac{A_{i+1}}{A_i} \hspace{3cm} (5)$$

where $y(\infty)$ denotes steady state of $y(t)$. The ratio of two successive amplitudes A_{i+1}/A_i is measure of $y(t)$ decaying, where $i=1...N$, and N is half of the number of $y(\infty)$ crossings by $y(t)$ (Fig. 2b). A time-domain performance measure is the settling time t_s, i.e. the time after which the output $y(t)$ remains within $\pm\varepsilon\%$ of its final value (Fig. 2a); typically $\varepsilon=[1\%\div5\%]y(\infty)$, $\delta_{DR}\in(1:4;1:2)$, $\eta_{\max}\in(0\%;50\%)$. Fig. 2c depicts underdamped (curve 1), overdamped (curve 2) and critically damped (curve 3) closed-loop step responses.
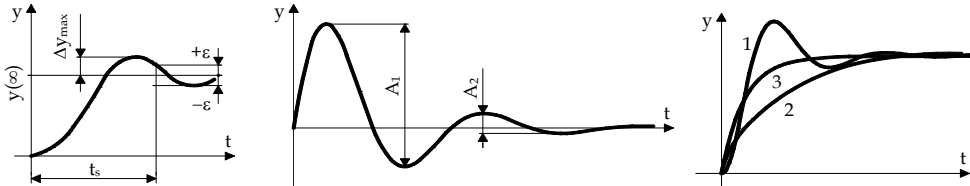

Fig. 2. Performance measures: δ_{DR}, t_s, $\eta_{\max}$ and $e(\infty)$; a) setpoint step response; b) load disturbance step response; c) over-, critically- and underdamped closed-loop step-responses

2.4 Model-free PID controller design techniques with guaranteed performance

Model-free tuning PID controller techniques are used if plant dynamics is not complicated (without oscillations, vibrations, large overshoots) or if plant modelling is time demanding, uneconomical or even unfeasible. To find PID controller coefficients, instead of a full model usually 2-4 characteristic plant parameters are used obtained from the relay test.

2.4.1 Tuning rules based on critical parameters of the plant

Consider the closed-loop in Fig. 1 with proportional controller. If the controller gain K is successively increased until the process variable oscillates with constant amplitudes, critical parameters can be specified: the period of oscillations T_c and the corresponding gain K_c. If the controller (4a) is considered, coefficients of P, PI and PID controllers are calculated according to Tab. 2, where $\omega_c=2\pi/T_c$ is critical frequency of the plant.

No.	Design method, year	Cont-roller	K	T_i	T_d	Performance or response
1.	(Ziegler & Nichols, 1942)	P	$0{,}5K_c$	-	-	Quarter decay ratio
2.	(Ziegler & Nichols, 1942)	PI	$0{,}45K_c$	$0{,}8T_c$	-	Quarter decay ratio
3.	(Ziegler & Nichols, 1942)	PID	$0{,}6K_c$	$0{,}5T_c$	$0{,}125T_c$	Quarter decay ratio
4.	(Pettit & Carr, 1987)	PID	K_c	$0{,}5T_c$	$0{,}125T_c$	Underdamped
5.	(Pettit & Carr, 1987)	PID	$0{,}67K_c$	T_c	$0{,}167T_c$	Critically damped
6.	(Pettit & Carr, 1987)	PID	$0{,}5K_c$	$1{,}5T_c$	$0{,}167T_c$	Overdamped
7.	(Chau, 2002)	PID	$0{,}33K_c$	$0{,}5T_c$	$0{,}333T_c$	Small overshoot
8.	(Chau, 2002)	PID	$0{,}2K_c$	$0{,}55T_c$	$0{,}333T_c$	Without overshoot
9.	(Bucz, 2011)	PID	$0{,}54K_c$	$0{,}79T_c$	$0{,}199T_c$	Overshoot $\eta_{\max}\leq20\%$
10.	(Bucz, 2011)	PID	$0{,}28K_c$	$1{,}44T_c$	$0{,}359T_c$	Settling time $t_s\leq13/\omega_c$

Table 2. Controller tuning based on critical parametres of the plant

Rules No. 1 – 3 represent the famous Ziegler-Nichols frequency-domain method with fast rejection of the disturbance $d(t)$ for $\delta_{DR}=1:4$ (Ziegler & Nichols, 1942). Related methods (No.

4 – 10) use various weighing of critical parameters thus allowing to vary closed-loop performance requirements. Methods (No. 1 – 10) are applicable for various plant types, easy-to-use and time efficient.

2.4.2 Specification of critical parameters of the plant using relay experiment

To quickly determine critical parameters K_c and T_c, industrial autotuners apply a relay test (Rotach, 1984) either with ideal relay (IR) or a relay with hysteresis (HR). In the loop in Fig. 1 when adjusting the setpoint w(t) in manual mode and switching SW into „3", a stable limit cycle around y(∞) arises. Due to switching between the levels –M, +M, G(s) is excited by a periodic rectangular signal u(t), (Fig. 3a). Then, ω_c and K_c can be calculated from

$$\omega_c = \frac{2\pi}{T_c} \; ; \;\; K_{c\_IR} = \frac{4M}{\pi A_c} \; ; \;\; K_{c\_HR} = \frac{4(M - 0{,}5\Delta_{DB})}{\pi A_c} \tag{6}$$

where the period and amplitude of oscillations T_c and A_c, respectively, can be obtained from a record of y(t) (Fig. 3b); Δ_{DB} is the width of the hysteresis. Relay amplitude M is usually adjusted at 3%÷10% of the control action limit. A relay with hysteresis is used if y(t) is corrupted by measurement noise n(t) (Yu, 2006); the critical gain is calculated using (6c).
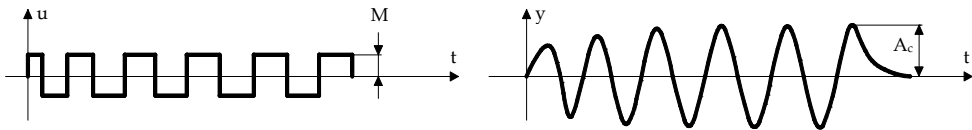

Fig. 3. A detailed view of u(t) and y(t) to determine critical parameters K_c and T_c

2.5 Model-based PID controller design with guaranteed performance

Steday-state and dynamic properties of real processes are described by simple FOPDT, IPDT, FOLIPDT or SOPDT models. Model parameters further used to calculate PID controller coefficients can be found e.g. from the plant step responses (Fig. 4 and 5).

2.5.1 Specification of FOPDT, IPDT and FOLIPDT plant model parameters

According to Fig. 1, the plant step response is obtained by switching SW into „2" and performing a step change in u(t). Plant model parameters are obtained by evaluating the particular step response (Fig. 4).
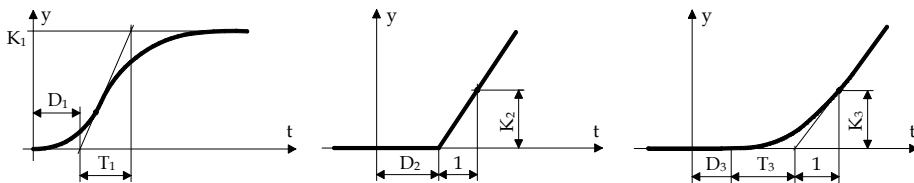

Fig. 4. Typical step responses of a) FOPDT; b) IPDT and c) FOLIPDT models

From the read-off parameters, transfer functions of individual models have been obtained

$$G_{FOPDT}(s) = \frac{K_1 e^{-D_1 s}}{T_1 s + 1} \; ; \; G_{IPDT}(s) = \frac{K_2 e^{-D_2 s}}{s} \; ; \; G_{FOLIPDT}(s) = \frac{K_3 e^{-D_3 s}}{s(T_3 s + 1)} \qquad (7)$$

2.5.2 Tuning formulae for FOPDT models

FOPDT models (7a) are used for chemical processes, thermal systems, manufacturing processes etc. Corresponding P, PI and PID coefficients are calculated using formulae in Tab. 3.

No.	Design method, year, control purpose	Cont-roller	K	T_i	T_d	Performance
11.	(Ziegler & Nichols, 1942)	P	$1/\kappa_1$	-	-	Quarter decay ratio (δ_{DR}=1:4)
12.		PI	$0,9/\kappa_1$	$3D_1$	-	
13.		PID	$1,2/\kappa_1$	$2D_1$	$0,5D_1$	
14.	(Chien et al., 1952), Regulator tuning	PI	$0,6/\kappa_1$	$4D_1$	-	η_{max}=0%, $D_1/T_1 \in (0,1;1)$
15.		PID	$0,95/\kappa_1$	$2,38D_1$	$0,42D_1$	
16.		PI	$0,7/\kappa_1$	$2,33D_1$	-	η_{max}=20%, $D_1/T_1 \in (0,1;1)$
17.		PID	$1,2/\kappa_1$	$2D_1$	$0,42D_1$	
18.	(Chien et al., 1952), Servo tuning	PI	$0,35/\kappa_1$	$1,17D_1$	-	η_{max}=0%, $D_1/T_1 \in (0,1;1)$
19.		PID	$0,6/\kappa_1$	D_1	$0,5D_1$	
20.		PI	$0,6/\kappa_1$	D_1	-	η_{max}=20%, $D_1/T_1 \in (0,1;1)$
21.		PID	$0,95/\kappa_1$	$1,36D_1$	$0,47D_1$	
22.	(ControlSoft Inc., 2005)	PID	$2/K_1$	T_1+D_1	$max(D_1/3;T_1/6)$	Slow loop
23.		PID	$2/K_1$	T_1+D_1	$min(D_1/3;T_1/6)$	Fast loop

Table 3. PID tuning rules based on FOPDT model; $\kappa_1 = K_1 D_1 / T_1$ is the normed process gain

Formulae No. 11 – 13 represent the time-domain (or reaction curve) Ziegler-Nichols method (Ziegler & Nichols, 1942) and usually give higher open-loop gains than the frequency-domain version. Algorithms by Chien-Hrones-Reswick provide different settings for setpoint regulation and disturbance rejection for two representative maximum overshoot values.

2.5.3 Tuning formulae for IPDT and FOLIPDT models

While dynamics of slow industrial processes (polymer production, heat exchangers) can be described by IPDT model (7b), electromechanic subsystems of turning machines and servodrives are typical examples for using FOLIPDT model (7c).

No.	Design method, year, model	Cont-roller	K	T_i	T_d	Perfor-mance
24.	(Haalman, 1965), IPDT	P	$0,66/(K_2 D_2)$	-	-	M_s=1,9
25.	(Ziegler & Nichols, 1942), IPDT	PI	$0,9/(K_2 D_2)$	$3,33D_2$	-	δ_{DR}=1:4
26.	(Ford, 1953), IPDT	PID	$1,48/(K_2 D_2)$	$2D_2$	$0,37D_2$	δ_{DR}=1:2,7
27.	(Coon, 1956), FOLIPDT	P	$x_3/[K_3(D_3+T_3)]$	-	-	δ_{DR}=1:4
28.	(Haalman, 1965), FOLIPDT	PD	$0,66/(K_3 D_3)$	-	T_3	M_s=1,9

Table 4. Tuning rules based on IPDT and FOLIPDT model parameters

According to Haalman (rules No. 24 and 28), controller transfer function $G_R(s)=L(s)/G(s)$, where $L(s)=0{,}66e^{-Ds}/(Ds)$ is the ideal loop transfer function guaranteeing maximum closed-loop sensitivity $M_s=1{,}9$ to disturbance $d(t)$, (see subsection 2.8.1). For various $G(s)$, various controller structures are obtained. The gain K in rule No. 27 depends on the normed time delay $\upsilon_3=D_3/T_3$ of the FOLIPDT model; for corresponding couples hold: $(\upsilon_3;x_3)=\{(0{,}02;5),$ $(0{,}053;4);\ (0{,}11;3);\ (0{,}25;2{,}2);\ (0{,}43;1{,}7);\ (1;1{,}3);\ (4;1{,}1)\}$. Due to integrator contained in IPDT and FOLIPDT models, I-term in the controller structure is needed just to achieve zero steady-state error $e(\infty)$ under steady-state disturbance $d(\infty)$.

2.5.4 Tuning formulae for SOPDT plant models

Flexible systems in wood processing industry, automotive industry, robotis, shocks and vibrations damping are often modelled by SOSPTD models with transfer functions

$$G_{SOPDT}(s)=\frac{K_4 e^{-D_4 s}}{(T_4 s+1)(T_5 s+1)}\ ;\ \ G_{SOPDT}(s)=\frac{K_6 e^{-D_6 s}}{T_6^2 s^2+2\xi_6 T_6 s+1} \tag{8}$$

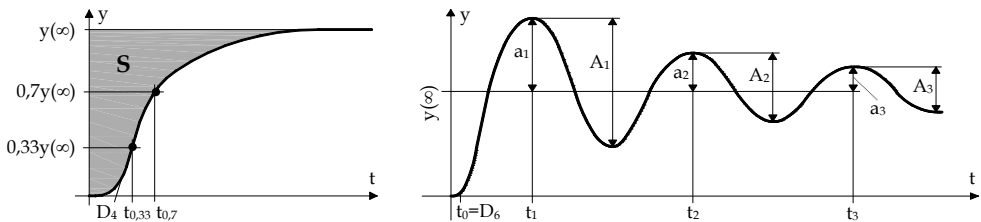For SOPDT model (8b), the relative damping $\xi_6\in(0;1)$ indicates oscillatory step response.

Fig. 5. Step response of SOPDT model: a) non-oscillatory, b) oscillatory

If $\xi_6>1$, SOPDT model (8a) is used; its parameters are found from the non-oscillatory step response in Fig. 5a using the following relations

$$T_{4,5}=\frac{1}{2}\left(C_2\pm\sqrt{C_2^2-4C_1^2}\right);\ D_4=\frac{t_{0,33}}{0{,}516}-\frac{t_{0,7}}{1{,}067}\ ;\ \ C_1=\frac{(t_{0,33}-t_{0,7})}{1{,}259}\ ;\ \ C_2=\frac{S}{y(\infty)}-D_4 \tag{9}$$

where $S=K_4(T_4+T_5+D_4)$ denotes the area above the step response of $y(t)$, and $y(\infty)$ is its steady-state value. Parameters of the SOPDT model (8b) can be found from evaluation of 2-4 periods of step response oscillations (Fig. 5b) using following rules (Vítečková, 1998)

$$\xi_6=\frac{-\ln\dfrac{a_{i+1}}{a_i}}{\sqrt{\pi^2+\ln^2\dfrac{a_{i+1}}{a_i}}}\ ;\ \ T_6=\frac{\sqrt{1-\xi_6^2}}{\pi N}(t_{N+1}-t_1)\ ;\ \ D_6=\frac{1}{N}\left[\sum_{i=1}^{N}t_i-\frac{N+1}{2}(t_{N+1}-t_1)\right] \tag{10}$$

Quality of identification improves with increasing number of read-off amplitudes N. If N>2 several values ξ_6, T_6 and D_6 are obtained and their average is taken for further calculations. Tab. 5 summarizes useful tuning formulae for both oscillatory and non-oscillatory systems with SOPDT model properties.

No.	Method, year	Cont-roller	K	T_i	T_d	Performance for
29.	(Suyama, 1992)	PID	$\dfrac{T_4+T_5}{2K_4D_4}$	T_4+T_5	$\dfrac{T_4T_5}{T_4+T_5}$	Closed-loop step response overshoot η_{max}=10%
30.	Vítečková, (1999),	PID	$x_4\dfrac{T_4+T_5}{K_4D_4}$	T_4+T_5	$\dfrac{T_4T_5}{T_4+T_5}$	Overdamped plants; $T_5>T_4$ η_{max}=0%: x_4=0,368 η_{max}=30%: x_4=0,801
31.	Vítečková et al., (2000)	PID	$\dfrac{x_6\xi_6T_6}{K_6D_6}$	$2\xi_6T_6$	$\dfrac{T_6}{2\xi_6}$	Underdamped plants (0,5<ξ_6≤1) η_{max}=0%: x_6=0,736 η_{max}=30%: x_6=1,602
32.	(Wang & Shao, 1999)	PID	$\dfrac{x_6\xi_6T_6}{K_6D_6}$	$2\xi_6T_6$	$\dfrac{T_6}{2\xi_6}$	[G_M=2, ϕ_M=45°]: x_6=1,571 [G_M=5, ϕ_M=72°]: x_6=0,628
33.	(Chen et al., 1999)	PID	$\dfrac{x_6\xi_6T_6}{K_6D_6}$	$2\xi_6T_6$	$\dfrac{D_6}{2\xi_6}$	[G_M;ϕ_M;M_s]=[3,14;61,4°;1]: x_6=1,0 [G_M;ϕ_M;M_s]=[1,96;44,1°;1,5]: x_6=1,6

Table 5. Tuning rules based on SOPDT model parameters

2.6 PID controller design based on optimization techniques

Optimal PID controller tuning can be found by minimizing the performance index

$$I(K,T_i,T_d) = \int_0^\infty \left[t^n e(K,T_i,T_d,t) \right]^2 dt \qquad (11)$$

Its particular cases are known as integral square error (ISE) for n=0; integral squared time weighed error (ISTE) for n=1, and integral squared time-squared weighed error (IST²E) for n=2. Some tuning formulae for PID controller in form (4a) are shown in Tab. 6. Settling time t_s in rules No. 40 and 41 is affected by D_2.

No.	Method, year, model	K	T_i	T_d	Performance
34.	(Zhuang & Atherton,	$1{,}473v_1^{0{,}970}/K_1$	$0{,}897T_1v_1^{0{,}753}$	$0{,}550T_1v_1^{0{,}948}$	Minimum ISE
35.	1993), FOPDT model,	$1{,}468v_1^{0{,}970}/K_1$	$1{,}062T_1v_1^{0{,}725}$	$0{,}443T_1v_1^{0{,}939}$	Minimum ISTE
36.	$v_1\in\langle0{,}1;1\rangle$	$1{,}531v_1^{0{,}960}/K_1$	$1{,}030T_1v_1^{0{,}746}$	$0{,}413T_1v_1^{0{,}933}$	Minimum IST²E
37.	(Zhuang & Atherton,	$1{,}524v_1^{0{,}735}/K_1$	$0{,}885T_1v_1^{0{,}641}$	$0{,}552T_1v_1^{0{,}851}$	Minimum ISE
38.	1993), FOPDT model,	$1{,}515v_1^{0{,}730}/K_1$	$1{,}045T_1v_1^{0{,}598}$	$0{,}444T_1v_1^{0{,}847}$	Minimum ISTE
39.	$v_1\in\langle1{,}1;2\rangle$	$1{,}592v_1^{0{,}705}/K_1$	$1{,}045T_1v_1^{0{,}597}$	$0{,}414T_1v_1^{0{,}850}$	Minimum IST²E
40.	(Wang a Cluett, 1997),	$0{,}9588/[K_2D_2]$	$3{,}0425D_2$	$0{,}3912D_2$	t_s=D_2
41.	IPDT model	$0{,}3144/[K_2D_2]$	$11{,}1637D_2$	$0{,}1453D_2$	t_s=$5D_2$

Table 6. Tuning rules based on minimizing performance indices

2.7 PID controller setting for unstable FOPDT models

Minimization of performance indices can be applied also for unstable FOPDT models

$$G_{FOPDT\_US}(s) = \frac{K_1 e^{-D_1 s}}{T_1 s - 1} \qquad (12)$$

leading to simple tuning rules for PID controller (4a) (No. 42 – 44 in Tab. 7). Tuning rules No. 45 and 46 for PID controller (4c) show that settling time t_s increases with growing normed time delay $v_1=D_1/T_1$ of the FOPDT model (12).

No.	Method, year	K	T_i	T_d	T_f	Performance
42.	(Visoli, 2001),	$1{,}37v_1/K_1$	$2{,}42T_1v_1^{1,18}$	$0{,}60T_1$	-	Minimum ISE
43.	Regulator	$1{,}37v_1/K_1$	$4{,}12T_1v_1^{0,90}$	$0{,}55T_1$	-	Minimum ISTE
44.	tuning	$1{,}70v_1/K_1$	$4{,}52T_1v_1^{1,13}$	$0{,}50T_1$	-	Minimum IST²E
45.	(Chandrashekar	$10{,}3662/K_1$	$0{,}3874T_1$	$0{,}0435T_1$	$0{,}0134T_1$	$t_s=0{,}1T_1$: $v_1=0{,}1$
46.	et al., 2002)	$2{,}0217/K_1$	$4{,}65T_1$	$0{,}2366T_1$	$0{,}0696T_1$	$t_s=0{,}8T_1$: $v_1=0{,}5$

Table 7. Tuning rules for unstable FOPDT model

Using tuning methods shown in Tab. 2 – 7, achieved performance is a priori given by the chosen metod (e.g. a quarter decay ratio if using Ziegler-Nichols methods No. 11 – 13 in Tab. 3), or guaranteed performance however not specified by the designer (e.g. in Chen method No. 33 in Tab. 5, a gain margin $G_M=1{,}96$, a phase margin $\phi_M=44{,}1°$, and a maximum peak of the sensitivity to disturbance d(t) $M_s=1{,}5$).

2.8 PID controller design for specified performance
These methods provide tuning rules are based on a single tuning parameter that enables to systematically affect closed-loop performance by step response shaping.

2.8.1 Performance measures used as a PID tuning parameter
Most frequent parameters for tuning PID controllers are following performance measures (Åström & Hägglund, 1995):
- ϕ_M and G_M: phase and gain margins, respectively,
- M_s and M_t: maximum peaks of sensitivity $S(j\omega)$ and complementary sensitivity $T(j\omega)$ magnitudes, respectively,
- λ: required closed-loop time constant.

If a controller $G_R(j\omega)$ guarantees that $|S(j\omega)|$ or $|T(j\omega)|$ do not overrun prespecified values M_s or M_t, respectively, defined by

$$M_s = \sup_{\omega}\left|S(j\omega)\right| = \sup_{\omega}\left|\frac{1}{1+L(j\omega)}\right|; \quad M_t = \sup_{\omega}\left|T(j\omega)\right| = \sup_{\omega}\left|\frac{L(j\omega)}{1+L(j\omega)}\right| \tag{13}$$

over $\omega\in\langle 0,\infty)$, then the Nyquist plot $L(j\omega)$ of the open-loop $L(s)=G(s)G_R(s)$ avoids the respective circle M_S or M_T , each given by the their center and radius as follows

$$C_S = \left[-1, j0\right], \ R_S = \frac{1}{M_s}; \quad C_T = \left[-\frac{M_t^2}{M_t^2-1}, j0\right], \ R_T = -\frac{M_t}{\left|1-M_t^2\right|} \tag{14}$$

If $L(j\omega)$ avoids entering the circles corresponding to M_S or M_T, a safe distance from the point C_S is kept (Fig. 6a). Typical $|S(j\omega)|$ and $|T(j\omega)|$ plots for properly designed controller are plotted in Fig. 6b. The disturbance d(t) is sufficiently rejected if $M_s\in(1{,}2;2)$. The reference w(t) is properly tracked by the process output y(t) if $M_t\in(1{,}3;2{,}5)$. With further increasing of M_t the closed-loop tends to be oscillatory.
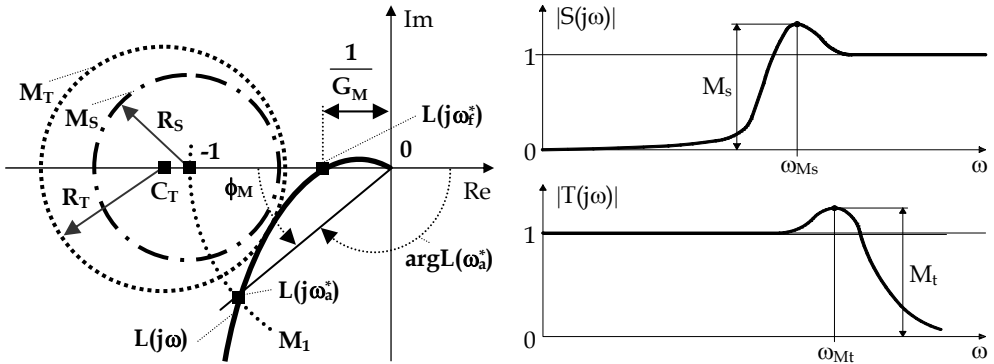
Fig. 6. a) Definition and geometrical interpretation of ϕ_M and G_M in the complex plane; b) Sensitivity and complementary sensitivity magnitudes $|S(j\omega)|$, $|T(j\omega)|$ and performance measures M_s, M_t

From Fig. 6a results, that increasing open-loop phase margin ϕ_M causes moving the gain crossover $L(j\omega_a^*)$ lying on the unit circle M_1 away from the critical point (-1,j0). Increasing open-loop gain margin G_M causes moving the phase crossover $L(j\omega_f^*)$ away from (-1,j0). Therefore, parameters ϕ_M or G_M given by

$$\phi_M = 180° + \arg L(\omega_a^*); \quad G_M = \frac{1}{\left|L(j\omega_f^*)\right|} \tag{15}$$

are frequently used performance measures, their typical values are $\phi_M \in (20°;90°)$, $G_M \in (2;5)$. Relations between them are given by following inequalities

$$\phi_M \geq 2\arcsin\left(\frac{1}{2M_s}\right); \quad \phi_M \geq 2\arcsin\left(\frac{1}{2M_t}\right); \quad G_M \geq \frac{M_s}{M_s-1}; \quad G_M \geq 1+\frac{1}{M_t} \tag{16}$$

The point at which the Nyquist plot $L(j\omega)$ touches the M_T circle defines the closed-loop resonance frequency ω_{Mt}.

2.8.2 Tuning formulae with performance specification

Table 8 shows open formulae for PID controller design. The coefficients tuning is carried out with respect to closed-loop performance specification. Rules No. 47 – 49 consider tuning of ideal PID controller (4a). To apply the Rotach method, knowledge of the plant magnitude $|G(j\omega)|$ is supposed as well as of the roll-off of $\arg G(\omega)$ at $\omega = \omega_{Mt}$, where the maximum peak M_t of the complementary sensitivity is required. Method No. 50 is based on so-called λ-tuning, with the resulting closed-loop expressed as a 1st order system with time constant λ; this rule considers a real PID controller (4b) with filtering constant in the derivative part $T_f = T_d/N = 0,5\lambda D_1/(1+D_1)$ where λ is to be chosen to meet following conditions: $\lambda > 0,25D_1$; $\lambda > 0,25T_1$ (Morari & Zafiriou, 1989). The λ-tuning technique is used also in the rule No. 51 to design interaction PI controller.

No.	Design method, year, model	K	T_i	T_d
47.	(Hang & Åström, 1988), Non-model	$K_c \sin\phi_M$	$\dfrac{T_c(1-\cos\phi_M)}{\pi \sin\phi_M}$	$\dfrac{T_c(1-\cos\phi_M)}{4\pi \sin\phi_M}$
48.	(Rotach, 1994), Non-model	$\dfrac{M_t|G(j\omega_{Mt})|}{\sqrt{M_t^2-1}}$	$\dfrac{-2}{\omega_{Mt}^2\left(\dfrac{d\left[\arg G(\omega_{Mt})\right]}{d\omega_{Mt}}\right)}$	$-\dfrac{1}{2}\dfrac{d\left[\arg G(\omega_{Mt})\right]}{d\omega_{Mt}}$
49.	(Wojsznis et al., 1999), FOPDT	$\dfrac{K_c \cos\phi_M}{G_M}$	$\dfrac{T_c}{\pi}\left(tg\phi_M+\sqrt{1+tg^2\phi_M}\right)$	$\dfrac{T_c}{4\pi}\left(tg\phi_M+\sqrt{1+tg^2\phi_M}\right)$
50.	(Morari & Zafiriou, 1989), FOPDT	$\dfrac{T_1+0{,}5D_1}{K_1(\lambda+D_1)}$	$T_1+\dfrac{1}{2}D_1$	$\dfrac{T_1 D_1}{2T_1+D_1}$
51.	(Chen & Seborg, 2002), FOPDT	$\dfrac{T_1 D_1+2T_1\lambda-\lambda^2}{K_1(\lambda+D_1)^2}$	$\dfrac{T_1 D_1+2T_1\lambda-\lambda^2}{T_1+D_1}$	-

Table 8. PID design formulae for specified performance based on tuning parameters ϕ_M, G_M, M_t and λ

2.8.3 Performance evaluation

Phase margin ϕ_M is the most wide-spread performance measure in PID controller design. Maximum overshoot η_{max} and settling time t_s of the closed-loop step response are related with ϕ_M according to Reinisch relations

$$\eta_{\max}=\begin{cases}-0{,}91\phi_M+64{,}55 & for\ \phi_M\in\langle 38°;71°\rangle \\ -1{,}53\phi_M+88{,}46 & for\ \phi_M\in\langle 12°;38°\rangle\end{cases};\ \eta_{\max}=100e^{-2\pi b^2 M_t};\ t_s\in\left(\frac{\pi}{\omega_a^*},\frac{4\pi}{\omega_a^*}\right) \quad (17)$$

valid for 2nd order closed-loop with relative damping $\xi\in(0{,}25;0{,}65)$ where ω_a^* is the gain crossover frequency (Hudzovič, 1982). Relations

$$\eta_{\max}\le 100\frac{1.18M_t-|T(0)|}{|T(0)|}\ [\%];\ t_s\approx\frac{3}{\omega_a^*}\ for\ M_t\in(1{,}3;1{,}5) \quad (18)$$

(Hudzovič, 1982); (Grabbe et al., 1959-61) are general for any order of the closed-loop T(s); if the controller has the integral part then |T(0)|=|T(ω=0)|=1.

The engineering practice is persistently demanding for PID controller design methods simultaneously guaranteeing several performance criteria, especially maximum overshoot η_{max} and settling time t_s. However, we ask the question: how to suitably transform the above-mentioned engineering requirements into frequency domain specifications applicable for PID controller coefficients tuning? The response can be found in Section 3 where a novel original PID controller design method is presented.

3. Advanced PID controller design method based on sine-wave identification

The presented method is applicable for linear stable SISO systems even with unknown mathematical model. The control objective is to provide required maximum overshoot η_{max} and settling time t_s of the process variable $y(t)$. The method enables the designer to prescribe η_{max} and t_s within following ranges (Bucz et al., 2010b, 2010c), (Bucz, 2011)

- $\eta_{max} \in \langle 0\%; 90\% \rangle$ and $t_s \in \langle 6,5/\omega_c; 45/\omega_c \rangle$ for systems without integrator,
- $\eta_{max} \in \langle 9,5\%; 90\% \rangle$ and $t_s \in \langle 11,5/\omega_c; 45/\omega_c \rangle$ for systems with integrator,

where ω_c is the plant critical frequency. The PID controller design provides guaranteed phase margin ϕ_M. The tuning rule parameter is a suitably chosen point of the plant frequency response obtained by a sine-wave signal with excitation frequency ω_n. The designed controller then moves this point into the gain crossover with the required phase margin ϕ_M. With respect to engineering requirements, the pair $(\omega_n; \phi_M)$ is specified on the closed-loop step response in terms of η_{max} and t_s according to parabolic dependencies in Fig. 11 and Fig. 14-16. A multipurpose loop for the proposed sine-wave method is in Fig. 7.
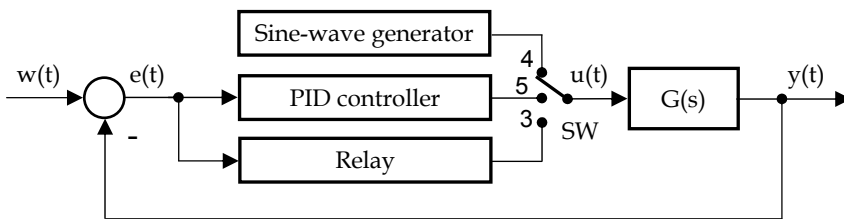
Fig. 7. Multipurpose loop for identification and control using the sine-wave method

3.1 Plant identification by a sinusoidal excitation input

By switching SW into "4", the loop in Fig. 7 opens; a stable plant with unknown model $G(s)$ is excited by a persistent sinusoid $u(t)=U_n\sin(\omega_n t)$ (Fig. 8a) where U_n denotes the amplitude and ω_n excitation frequency. The plant output $y(t)=Y_n\sin(\omega_n t+\varphi)$ is also a persistent sinusoid with the same frequency ω_n, amplitude Y_n and phase shift φ with respect to the input excitation sinusoid (Fig. 8b). From the stored records of $y(t)$ and $u(t)$ it is possible to read-off the amplitude Y_n and phase shift φ_n and thus to identify a particular point of the plant frequency response $G(j\omega)$ under excitation frequency ω_n with coordinates $G \equiv G(j\omega_n)$

$$G(j\omega_n) = \left| G(j\omega_n) \right| e^{j\arg G(\omega_n)} = \frac{Y_n(\omega_n)}{U_n(\omega_n)} e^{j\arg G(\omega_n)} \tag{19}$$

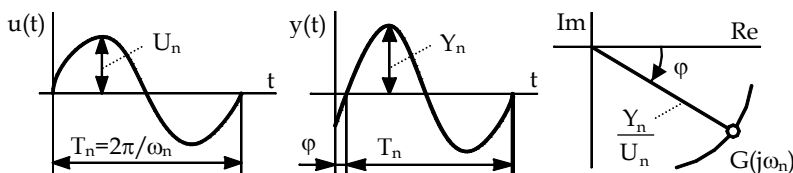where $\varphi = \arg G(\omega_n)$. The point $G(j\omega_n)$ can be plotted in the complex plane (Fig. 8c).

Fig. 8. Time responses of a) $u(t)$; b) $y(t)$, and c) location of $G(j\omega_n)$ in the complex plane

The output sinusoid amplitude Y_n can be affected by the amplitude U_n of the excitation sinusoid generated by the sine wave generator; it is recommended to use $U_n=3÷7\%u_{max}$. Identified plant parameters are represented by the triple $\{\omega_n, Y_n(\omega_n)/U_n(\omega_n), \varphi(\omega_n)\}$. In the SW position „4", identification is performed in the open-loop. Hence, this method is applicable only for stable plants. The excitation frequency ω_n is to be adjusted prior to identification and taken from the empirical interval (29) (Bucz et al., 2010a, 2010b, 2011).

3.2 Sine-wave method tuning rules

In the control loop in Fig. 7, let us switch SW in „5"and put the PID controller into manual mode. The closed-loop characteristic equation $1+L(j\omega)=1+G(j\omega)G_R(j\omega)=0$ at the gain crossover frequency ω_a^* can be broken down into the amplitude and phase conditions as follows

$$\left|G(j\omega_a^*)\right|\left|G_R(j\omega_a^*)\right| = 1; \quad \arg G(\omega_a^*) + \arg G_R(\omega_a^*) = -180° + \phi_M \tag{20}$$

where ϕ_M is the required phase margin, $L(j\omega_n)$ is the open-loop transfer function. Denote $\Theta = \arg G_R(\omega_a^*)$. We are searching for K, T_i and T_d of the ideal PID controller (4a). Comparing frequency transfer functions of the PID controller in parallel and polar forms

$$G_R(j\omega) = K + jK\left[T_d\omega - \frac{1}{T_i\omega}\right]; \quad G_R(j\omega) = \left|G_R(j\omega)\right|e^{j\Theta} = \left|G_R(j\omega)\right|\cos\Theta + j\left|G_R(j\omega)\right|\sin\Theta \tag{21}$$

coefficients of PID controller can be obtained from the complex equation

$$K + jK\left[T_d\omega_a^* - \frac{1}{T_i\omega_a^*}\right] = \frac{\cos\Theta}{\left|G(j\omega_a^*)\right|} + j\frac{\sin\Theta}{\left|G(j\omega_a^*)\right|}, \tag{22}$$

at $\omega=\omega_a^*$ using the substitution $|G_R(j\omega_a^*)|=1/|G(j\omega_a^*)|$ resulting from the amplitude condition (20a). The complex equation (22) is solved as a set of two real equations

$$K = \frac{\cos\Theta}{\left|G(j\omega_a^*)\right|}; \quad K\left[T_d\omega_a^* - \frac{1}{T_i\omega_a^*}\right] = \frac{\sin\Theta}{\left|G(j\omega_a^*)\right|} \tag{23}$$

where (23a) is a general rule for calculation of the controller gain K. Using (23a) and the ratio of integration and derivative times $\beta=T_i/T_d$ in (23b), a quadratic equation in T_d is obtained after some manipulations

$$T_d^2\left(\omega_a^*\right)^2 - T_d\omega_a^* tg\Theta - \frac{1}{\beta} = 0 \tag{24}$$

A positive solution of (24) yields the rule for calculating the derivative time T_d

$$T_d = \frac{tg\Theta}{2\omega_a^*} + \frac{1}{\omega_a^*}\sqrt{\frac{tg^2\Theta}{4} + \frac{1}{\beta}}; \quad \Theta = -180° + \phi_M - \arg G(\omega_a^*) \tag{25}$$

where $\Theta=\arg G_R(\omega_a^*)$ is found from the phase condition (20b). Thus, using the PID controller with coefficients $\{K;T_i=\beta T_d;T_d\}$, the identified point $G(j\omega_n)$ of the plant frequency response with coordinates (19) can be moved on the unit circle M_1 into the gain crossover $L_A \equiv L(j\omega_a^*)$; the required phase margin ϕ_M is guaranteed if the following identity holds between the excitation and amplitude crossover frequencies ω_n and ω_a^*, respectively

$$\omega_a^* = \omega_n \tag{26}$$

Thus

$$\left|G(j\omega_a^*)\right| = \left|G(j\omega_n)\right| ; \quad \arg G(\omega_a^*) = \arg G(\omega_n) = \varphi ; \quad \Theta = -180° + \phi_M - \varphi \tag{27}$$

and coordinates of the gain crossover L_A are

$$L_A \equiv L(j\omega_a^* \equiv j\omega_n) = \left[\left|L(j\omega_n)\right|, \arg L(\omega_n)\right] = \left[\left|1\right|, -180° + \phi_M\right] \tag{28}$$

Substituting (27a) and (27b) into (23a) and (23b), respectively, and (26) into (25a), tuning rules in Table 9 are obtained (Bucz et al., 2010a, 2010b, 2010c, 2011), (Bucz, 2011). Resulting PID controller coefficients guarantee required phase margin ϕ_M for $\beta=4$.

No.	Design method, year	Cont-roller	K	T_i	T_d	Range of Θ; $\Theta=-180°+\phi_M-\varphi$
52.	Sine-wave method, 2010	PI	$\dfrac{\cos\Theta}{\left|G(j\omega_n)\right|}$	$\dfrac{-1}{\omega_n tg\Theta}$	–	$\left(-\dfrac{\pi}{2};0\right)$
53.	Sine-wave method, 2010	PD	$\dfrac{\cos\Theta}{\left|G(j\omega_n)\right|}$	–	$\dfrac{1}{\omega_n}tg\Theta$	$\left(0;\dfrac{\pi}{2}\right)$
54.	Sine-wave method, 2010	PID	$\dfrac{\cos\Theta}{\left|G(j\omega_n)\right|}$	βT_d	$\dfrac{tg\Theta}{2\omega_n}+\dfrac{1}{\omega_n}\sqrt{\dfrac{tg^2\Theta}{4}+\dfrac{1}{\beta}}$	$\left(-\dfrac{\pi}{2};\dfrac{\pi}{2}\right)$

Table 9. PI, PD and PID controller tuning rules according to the sine-wave method

Note that PI controller tuning rules were derived for $T_d=0$, and PD tuning rules for $T_i\to\infty$ in (21a). The excitation frequency is taken from the interval (Bucz et al., 2011), (Bucz, 2011)

$$\omega_n \in \langle 0,2\omega_c;0,95\omega_c\rangle \tag{29}$$

obtained empirically by testing the sine-wave method on benchmark examples (Åström & Hägglund, 2000). Shifting the point $G(j\omega_n)=|G(j\omega_n)|e^{j\varphi}$ into the gain crossover $L_A(j\omega_n)$ on the unit circle M_1 is depicted in Fig. 9a.

3.3 Controller structure selection using the „triangle ruler" rule

The argument Θ appearing in tuning rules in Tab. 9 indicates, what angle is to be contributed to the identified phase φ by the controller at ω_n to obtain the resulting open-loop phase $(-180°+\phi_M)$ needed to provide the required phase margin ϕ_M. The working range of PID controller argument is the union of PI and PD controllers phase ranges symmetric with respect to $0°$

$$\Theta_{PID} \in \Theta_{PI} \cup \Theta_{PD} = \left(-90°,0°\right) \cup \left(0°,+90°\right) = \left(-90°,+90°\right) \tag{30}$$

The working range (30) can be interpreted by means of an imaginary transparent triangular ruler turned as in Fig. 9b; its segments to the left and right of the axis of symmetry represent the PD and PI working ranges, respectively. Put this ruler on Fig. 9a, the middle of the hypotenuse on the complex plane origin and turn it so that its axis of symmetry merges with the ray (0,G). Thus, the ruler determines in the complex plane the cross-hatched area representing the full working range of the PID controller argument. The controller type is chosen depending on the situation of the ray (0,L_A) forming the angle ϕ_M with the negative real halfaxis: situation of the ray (0,L_A) in the left-hand-sector suggests PD controller, and in the right-hand sector the PI controller. The case when the phase margin ϕ_M is achievable using both PI or PID controller is shown in Fig. 9b (Bucz et al., 2010b, 2011), (Bucz, 2011).
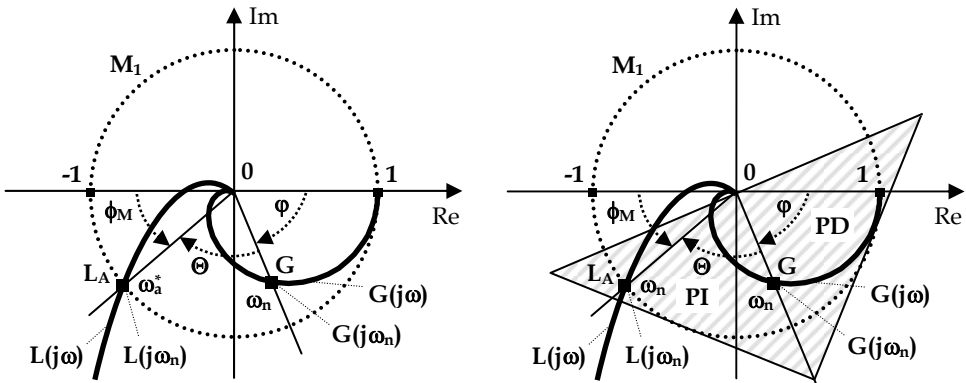
Fig. 9. a) Graphical interpretation of ϕ_M, ω_a^* and shifting G into L_A at $\omega_a^*=\omega_n$; b) controller structure selection with respect to location of G and L_A using the „triangle ruler" rule

3.4 Evaluation of closed-loop performance under the sine-wave type PID controller

This subsection answers the following question: how to transform required the maximum overshoot η_{max} and settling time t_s into the couple of frequency-domain parametres (ω_n,ϕ_M) needed for identification and PID controller coefficients tuning (Bucz, 2011)?

3.4.1 Systems without integrator

Looking for appropriate transformation $\Re$: (η_{max},t_s)$\rightarrow$(ω_n,ϕ_M) we have considered typical phase margins ϕ_M given by the set

$$\left\{\phi_{Mj}\right\} = \left\{20°,30°,40°,50°,60°,70°,80°,90°\right\} , \text{ j=1...8} \tag{31}$$

split into 5 equal sections $\Delta\omega_n=0,15\omega_c$; let us generate the set of excitation frequencies

$$\left\{\omega_{nk}\right\} = \left\{0,2\omega_c;0,35\omega_c;0,5\omega_c;0,65\omega_c;0,8\omega_c;0,95\omega_c\right\} , \text{ k=1...6} \tag{32}$$

Elements of (32) divided by the plant critical frequency ω_c determine the set of so-called excitation levels

$$\{\sigma_k = \omega_{nk}/\omega_c\} \Rightarrow \{\sigma_k\} = \{0,2;0,35;0,5;0,65;0,8;0,95\} \text{ , k=1...6} \tag{33}$$

Fig. 10 shows closed-loop step responses under PID controllers designed for the plant

$$G_1(s) = \frac{1}{(s+1)(0,5s+1)(0,25s+1)(0,125s+1)} \tag{34}$$

for three different phase margins ϕ_M=40°,60°,80° each on three excitation levels $\sigma_1=\omega_{n1}/\omega_c$=0,2; $\sigma_3=\omega_{n3}/\omega_c$=0,5 and $\sigma_5=\omega_{n5}/\omega_c$=0,8. Qualitative effect of ω_{nk} and ϕ_{Mj} on closed-loop step response is demonstrated.
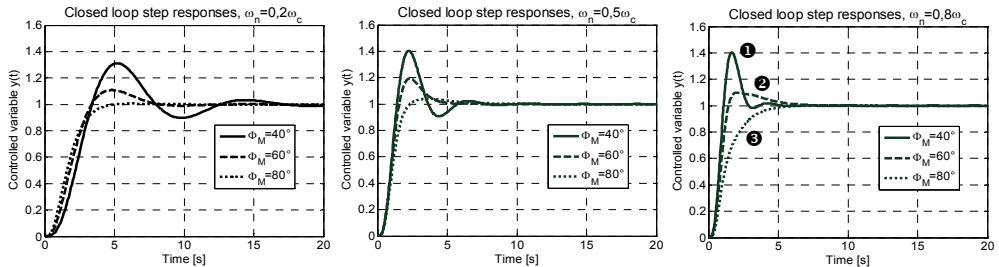
Fig. 10. Closed-loop step responses of $G_1(s)$ under PID controllers designed for various ϕ_M and ω_n

Achieving t_s and η_{max} was tested by designing PID controller for a vast set of benchmark examples (Åström & Hägglund, 2000) at excitation frequencies and phase margins expressed by a Cartesian product $\phi_{Mj} \times \omega_{nk}$ of (31) and (32) for j=1...8, k=1...6. Acquired dependencies η_{max}=f(ϕ_M, ω_n) and t_s=(ϕ_M, ω_n) are plotted in Fig. 11 (Bucz et al., 2010b, 2011).
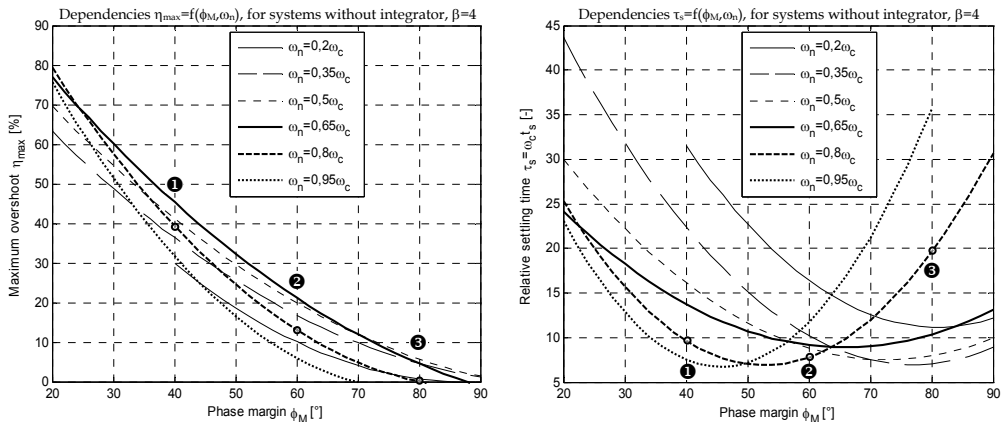
Fig. 11. Dependencies: a) η_{max}=f(ϕ_M, ω_n); b) τ_s=$\omega_c t_s$=f(ϕ_M, ω_n) for $\omega_{nk} \times \phi_{Mj}$, j=1...8, k=1...6 (relative settling time τ_s is t_s weighed by the critical frequency ω_c of the plant)

Considering (26) resulting from the assumptions of the engineering method, the settling time can be expressed by the relation

$$t_s = \frac{\gamma\pi}{\omega_n} \tag{35}$$

similar to (17c) (Hudzovič, 1989), γ is the curve factor of the step response. In (17c) valid for a 2nd order closed-loop, γ is from the interval (1;4) and depends on the relative damping (Hudzovič, 1989). In case of the proposed sine-wave method, γ varies in a considerably broader interval (0,5;16) found empirically, and strongly depends on ϕ_M, i.e. $\gamma = f(\phi_M)$ at the given excitation frequency ω_n. To examine closed-loop settling times of plants with various dynamics, it is advantageous to define the relative settling time (Bucz et al., 2011)

$$\tau_s = t_s \omega_c \tag{36}$$

Substituting $\omega_n = \sigma\omega_c$ into (35), the following relation for the relative settling time is obtained

$$t_s\omega_c = \frac{\pi}{\sigma}\gamma \;\Rightarrow\; \tau_s = \frac{\pi}{\sigma}\gamma \tag{37}$$

where t_s is related to the critical frequency ω_c. By substituting ω_c in (37) its left-hand side is constant for the given plant, independent of ω_n. Fig. 11b depicts (37b) empirically evaluated for different excitation frequencies ω_{nk}; it is evident that at every excitation level σ_k with increasing phase margin ϕ_M the relative settling time τ_s first decreases and after achieving its minimum τ_{s_min} it increases again. Empirical dependencies in Fig. 11 were approximated by quadratic regression curves and called B-parabolas. B-parabolas are a useful design tool to carry out the transformation $\Re:(\eta_{max},t_s)\rightarrow(\omega_n,\phi_M)$ that enables choosing appropriate values of phase margin and excitation frequencies ϕ_M and ω_n, respectively, to provide performance specified in terms of maximum overshoot η_{max} and settling time t_s (Bucz et al., 2011). Note that pairs of B-parabolas at the same level (Fig. 11a, Fig. 11b) are always to be used.

Procedure 1. Specification of ϕ_M and ω_n from η_{max} and t_s from B-parabolas prior to designing the controller

1. Set the PID controller into manual mode. Find the plant critical frequency ω_c using the multipurpose loop in Fig. 7 (SW in position „3").
2. From the required settling time t_s calculate the relative settling time $\tau_s = \omega_c t_s$.
3. On the vertical axis of the plot in Fig. 11b find the value of τ_s calculated in Step 2.
4. Choose the excitation level σ (e.g. $\sigma_5 = \omega_{n5}/\omega_c = 0,8$).
5. For τ_s, find the corresponding phase margin ϕ_M on the parabola $\tau_s = f(\phi_M,\omega_n)$ with the chosen excitation level found in Step 4.
6. Find ϕ_M from Step 5 on the horizontal axis of the plot in Fig. 11a.
7. For ϕ_M, find the corresponding maximum overshoot η_{max} on the parabola $\eta_{max} = f(\phi_M,\omega_n)$ with the chosen excitation level found in Step 4.
8. If the found η_{max} is inappropriate, repeat Steps 4 to 7 for other parabolas $\tau_s = f(\phi_M,\omega_n)$ and $\eta_{max} = f(\phi_M,\omega_n)$ corresponding to other levels $\sigma_k = \omega_{nk}/\omega_c$ (related with the choice $\sigma_5 = \omega_{n5}/\omega_c = 0,8$ for $\sigma_k = \{0,2;0,35;0,50;0,65;0,95\}$, k=1...4,6). Repeat until both the required performance measures η_{max} and t_s are satisfied.

9.   Calculate the excitation frequency ω_n according to the relation $\omega_n = \sigma \omega_c$ using the critical frequency ω_c (from Step 1) and the chosen excitation level σ (from Step 4).

Discussion

When choosing $\phi_M = 40°$ on the B-parabola corresponding to the excitation level $\sigma_5 = \omega_{n5}/\omega_c = 0,8$ (further denoted as $B_{0,8}$ parabola), maximum overshoot $\eta_{max} = 40\%$ and relative settling time $\tau_s \approx 10$ are expected. Point ❶ corresponding to these parameters is located on the left (falling) portion of $B_{0,8}$ yielding oscillatory step response (see response ❶ in Fig. 10c). If the phase margin increases up to $\phi_M = 60°$, the relative settling time decreases up to the point ❷ on the right (rising) portion of the $B_{0,8}$ parabola; the corresponding step response ❷ in Fig. 10c is weakly-aperiodic. For the phase margin $\phi_M = 80°$ the $B_{0,8}$ parabola indicates a zero maximum overshoot, the relative settling time $\tau_s = 20$ corresponds to the position ❸ on the $B_{0,8}$ parabola with aperiodic step response ❸ (Fig. 10c). If the maximum overshoot $\eta_{max} = 20\%$ is acceptable then $\phi_M = 53°$ yields the least possible relative settling time $\tau_s = 6,5$ on the given level $\sigma_5 = 0,8$ ("at the bottom" of $B_{0,8}$) (Bucz et al., 2011), (Bucz, 2011).

Procedure 2. PID controller design using the sine-wave engineering method

1.   From the required values (η_{max}, t_s) specify the couple $(\omega_n; \phi_M)$ using Procedure 1.
2.   Identify the plant using the sinusoidal excitation signal with frequency ω_n specified in Procedure 1. The switch SW is in position „4".
3.   Specify $\varphi = \arg G(\omega_n)$, and $|G(j\omega_n)|$. Calculate the controller argument Θ by substituting φ and ϕ_M into (27c); if Θ is within the range shown in the last column of Tab. 9, go to Step 4, if not, change $(\omega_n; \phi_M)$ and repeat Steps 1-3.
4.   Substitute the identified values $\varphi = \arg G(\omega_n)$, $|G(j\omega_n)|$ and specified ϕ_M into the tuning rules in Tab. 9 to calculate PID controller parameters.
5.   Adjust the resulting PID controller values, switch into automatic mode and complete the controller by switching SW into position „5".

Example 1

Using the sine-wave method, ideal PID controller (4a) is to be designed for the operating amplifier modelled by the transfer function $G_A(s)$

$$G_A(s) = \frac{1}{(T_A s + 1)^3} = \frac{1}{(0,01s + 1)^3} \tag{38}$$

The controller has to be designed for two values of the maximum overshoot of the closed-loop step response $\eta_{max1} = 30\%$ (Design No. 1) and $\eta_{max2} = 5\%$ (Design No. 2) and maximum relative settling time $\tau_s = 12$ in both cases.

Solution

1.   Critical frequency of the plant identified by the Rotach test is $\omega_c = 173,216$[rad/s] (the process is "fast"). The prescribed settling time is $t_s = \tau_s / \omega_c = 12/173,216$[s]=69,3[ms].
2.   For the Design No. 1 $(\eta_{max1}; \tau_s) = (30\%; 12)$, a suitable choice is $(\phi_{M1}; \omega_{n1}) = (50°; 0,5\omega_c)$ resulting from the $B_{0,5}$ parabola in Fig. 11. The performance in Design No. 2 $(\eta_{max2}; \tau_s) = (5\%; 12)$ can be achieved for $(\phi_{M2}; \omega_{n2}) = (70°; 0,8\omega_c)$ chosen from the $B_{0,8}$ parabola in Fig. 11.
3.   Identified points for the Designs No. 1 and No. 2 are $G_A(j0,5\omega_c) = 0,43e^{-j120°}$ and $G_A(j0,8\omega_c) = 0,19e^{-j165°}$, respectively. According to Fig. 12a, both points are located in the

Quadrant II of the complex plane, on the Nyquist plot $G_A(j\omega)$ (solid line) which verifies the identification.

4. Using the PID controller designed for $(\phi_{M1};\omega_{n1})=(50°;0,5\omega_c)$, the point $G_A(j0,5\omega_c)$ is moved into the gain crossover $L_{A1}(j0,5\omega_c)=1e^{-j130°}$ on the unit circle M_1, which verifies achieving the phase margin $\phi_{M1}=180°-130°=50°$ (dashed line in Fig. 12a). The point $G_A(j0,8\omega_c)$ has been moved into $L_{A2}(j0,8\omega_c)=1e^{-j110°}$ by the PID controller designed for $(\phi_{M2};\omega_{n2})=(80°;0,8\omega_c)$ yielding the phase margin $\phi_{M2}=180°-110°=70°$ (dotted line in Fig. 12a).

5. Achieved performance according to the closed-loop step response in Fig. 12b (dashed line) is $\eta_{max1}{}^*=29,7\%$, $t_{s1}{}^*=58,4[ms]$. Performance in terms of $\eta_{max2}{}^*=4,89\%$, $t_{s2}{}^*=60,5[ms]$ identified from the closed-loop step response in Fig. 12b (dotted line) fulfils the performance requirements.
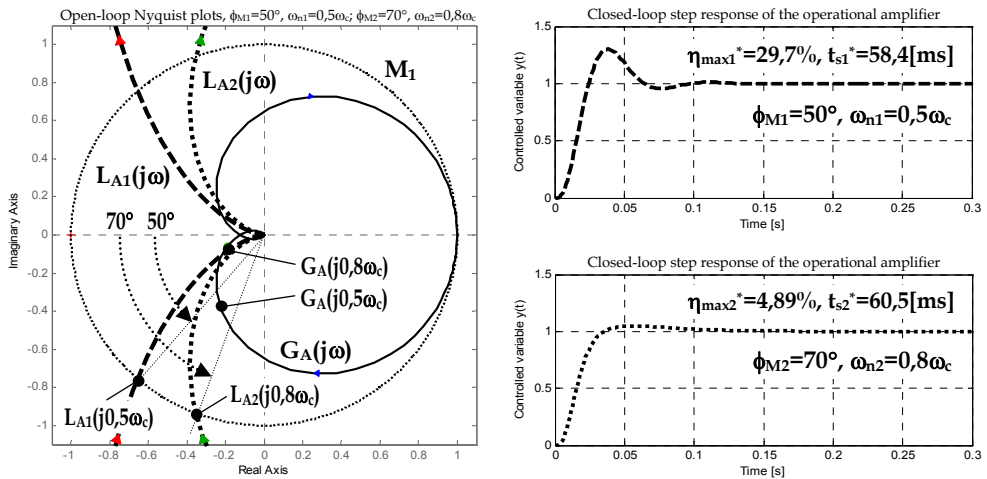
Fig. 12. a) Open-loop Nyquist plots; b) closed-loop step responses of the operational amplifier, required performance $\eta_{max1}=30\%$, $\eta_{max2}=5\%$ and $\tau_s=12$

3.4.2 Systems with time delay

The sine-wave method is applicable also for plants with time delay considered as difficult-to-control systems. It is a well-known fact, that the time delay D turns the phase at each frequency $\omega_n \in \langle 0,\infty)$ by $\omega_n D$ with respect to the delay-free system. For time delayed plants, phase condition of the sine-wave method (20b) is extended by additional phase $\phi_D=-\omega_n D$

$$\left(\varphi' + \varphi_D\right) + \Theta = -180° + \phi_M \tag{39}$$

where φ' is the phase of the delay-free system and

$$\varphi = \varphi' + \varphi_D \tag{40}$$

is the identified phase of the plant including the time delay. The added phase $\phi_D=-\omega_n D$ can be associated with the required phase margin ϕ_M

$$\varphi^{'} + \Theta = -180° + \left(\phi_M + \omega_n D\right) \tag{41}$$

The only modification in using the PID tuning rules in Tab. 9 is that increased required phase margin is to be specified (Bucz, 2011)

$$\phi_M^{'} = \phi_M + \omega_n D \tag{42}$$

and the controller working angle Θ is computed using the relation

$$\Theta = -180° - \varphi^{'} + \left(\phi_M + \omega_n D\right) \tag{43}$$

The phase delay $\omega_n D$ increases with increasing frequency of the sinusoidal signal ω_n.

To lessen the impact of time delay on closed-loop dynamics, it is recommended to use the smallest possible added phase $\varphi_D = -\omega_n D$.

Discussion

Time delay D can easily be specified during critical frequency identification as the time $D=T_y-T_u$, that elapses since the start of the test at time T_u until time T_y, when the system output starts responding to the excitation signal $u(t)$. A small added phase $\varphi_D=-\omega_n D$ due to time delay can be secured by choosing the smallest possible ω_n attenuating effect of D in (43) and subsequently in the PID controller design.

Therefore, when designing PID controller for time delayed systems according to Procedure 1, in Step 4 it is recommended to choose the lowest possible excitation level on the performance B-parabolas (most frequently ω_n/ω_c=0,2 resp. 0,35) and corresponding couples of B-parabolas in Fig. 11. Procedure 2 is used for plant identification and PID controller design. ϕ_M is specified from the given couple (η_{max};t_s) using the chosen couple of B-parabolas, however its increased value $\phi_M^{'}$ given by (42) is to be supplied in the design algorithm thus minimizing effect of the time delay on closed-loop dynamics.

Example 2

Using the sine-wave method, ideal PID controllers (4a) are to be designed for the distillation column modelled by the transfer function $G_B(s)$

$$G_B(s) = \frac{K_B e^{-D_B s}}{T_B s + 1} = \frac{1,11 e^{-6,5s}}{3,25s + 1} \tag{44}$$

Control objectives are the same as in Example 1.

Solution

1. Critical frequency of the plant is ω_c=0,3521[rad/s]. Based on comparison of critical frequencies, $G_B(s)$ is 500-times slower than $G_A(s)$. Required settling time is $t_s=\tau_s/\omega_c$= =12/0,3521[s]=34,08[s].
2. Because D_B/T_B=2>1, the plant is a so-called „dead-time dominant system". Due to a large the time delay, it is necessary to choose the lowest possible excitation frequency ω_n to minimize the added phase $\omega_n D_B$ in (43). Hence, for the required performance (η_{max2};τ_s)=(5%;12) (Design No. 2) we choose the $B_{0,2}$ parabolas in Fig. 11 at the lowest possible level ω_n/ω_c=0,2 to find (ϕ_{M2};ω_{n2})=(70°;0,2ω_c). The added phase is

$\omega_{n2}D_B(180°/\pi)=0,2\omega_cD_B(180°/\pi)=0,2.0,3521.6,5.180°/\pi=26,2°$, hence the phase supplied to the PID design algorithm is $\phi'_{M2}=\phi_{M2}+\omega_{n2}D_B(180°/\pi)=70°+26,2°=96,2°$ (instead of $\phi_{M2}=70°$ for a delay-free system). The required performance $(\eta_{max1};\tau_s)=(30\%;12)$ (Design No. 1) can be achieved by choosing $(\phi_{M1};\omega_{n1})=(55°;0,35\omega_c)$ from the $B_{0,35}$ parabolas in Fig. 11 (i.e. $\omega_n/\omega_c=0,35$). The phase margin $\phi'_{M1}=55°+45,9°$ supplied into the design algorithm was increased by $\omega_{n1}D_B(180°/\pi)=0,35\omega_cD_B(180°/\pi)=0,35.0,3521.6,5.180°/\pi==45,9°$ compared with $\phi_{M1}=55°$ in case of delay-free system.

3. Identified points $G_B(j0,35\omega_c)=1,03e^{-j23°}$ and $G_B(j0,2\omega_c)=1,09e^{-j13°}$ in Fig. 13a are located in the Quadrant I of the complex plane at the beginning of the frequency response $G_B(j\omega)$ (solid line). The point $G_B(j0,2\omega_c)$ (Design No. 2) was shifted by the PID controller to the open-loop gain crossover $L_{B2}(j0,2\omega_c)=1e^{-j110°}$ (dotted line in Fig. 13a). Note that L_{B2} has the same location in the complex plane as L_{A2} in Fig. 12a, however at a considerably lower frequency $\omega_{n2B}=0,2.0,3521=0,07[rad/s]$ compared to $\omega_{n2A}=0,8.173,216==138,6[rad/s]$ ($t_{s2\_B}^*=28,69[s]$ is almost 500 times larger than $t_{s2\_A}^*=0,0584[s]$ which demonstrates the key role of the excitation frequency ω_n in achieving required closed-loop dynamics). The identified point $G_B(j0,35\omega_c)$ (Design No. 1) was moved into the gain crossover $L_{B1}(j0,35\omega_c)=1e^{-j125°}$ (dashed line in Fig. 13a).

4. Achieved performances $(\eta_{max1}^*=18,6\%,\ t_{s1}^*=24,78[s]$, dashed line), $(\eta_{max2}^*=0,15\%$, $t_{s2}^*=28,69[s]$, dotted line) in terms of closed-loop step responses in Fig. 13b comply with the required performance specification.
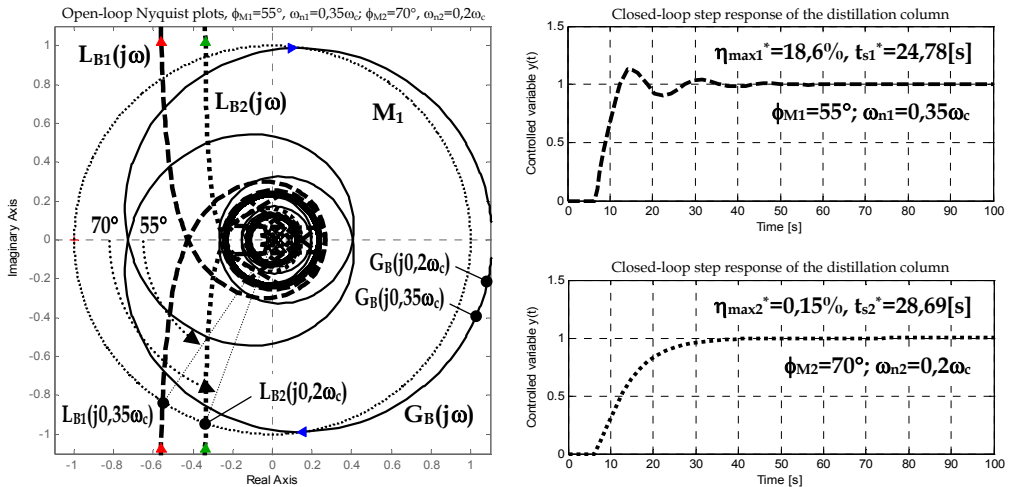

Fig. 13. a) Open-loop Nyquist plots; b) closed-loop step responses of the distillation column, required performance $\eta_{max1}=30\%$, $\eta_{max2}=5\%$ and $\tau_s=12$

3.4.3 Systems with 1st order integrator

By testing the sine-wave method on benchmark systems with 1st order integrator, the B-parabolas in Fig. 14 – 16 were obtained (for Cartesian product $\phi_{Mj}\times\omega_{nk}$ of sets (31) and (32), j=1...8, k=1...6 and three various ratios T_i/T_d: β=4, 8 and 12).

Discussion

Inspection of Fig. 14a, 15a and 16a reveals, that increasing β results in decreasing of the maximum overshoot η_{max}, narrowing of the B-parabolas of relative settling times $\tau_s=f(\phi_M,\omega_n)$ for each identification level ω_n/ω_c, and consequently settling time increasing. Consider e.g. the $B_{0,95}$ parabolas in Fig. 14b, Fig. 15b and Fig. 16b: if $\phi_M=70°$ and $\beta=4$, relative settling time is $\tau_s=30$, for $\beta=8$ it grows to $\tau_s=40$, and for $\beta=12$ even to $\tau_s=45$. If a 10% maximum overshoot is acceptable, then the standard interaction PID controller can be used with no need to use a setpoint filter; however a larger settling time is to be expected.

Procedure 1 is used to specify the performance in terms of (ϕ_M,ω_n) from (η_{max},t_s) using pertinent B-parabolas in Fig. 14 – 16. Procedure 2 is used for plant identification and PID controller design.

Example 3

Using the sine-wave method, design ideal PID controller for the flow valve modelled by the transfer function $G_C(s)$ (system with integrator and time delay)

$$G_C(s) = \frac{K_C e^{-D_C s}}{s(T_C s + 1)} = \frac{1,3 e^{-2,1s}}{s(7,51s + 1)} \tag{45}$$

Control objective is to provide the maximum overshoots of the closed-loop step response $\eta_{max1}=30\%$, $\eta_{max2}=20\%$ and a maximum relative settling time $\tau_s=20$.

Solution

1. Critical frequency of the plant identified by the Rotach test is $\omega_c=0,2407[rad/s]$. Then, the required settling time is $t_s=\tau_s/\omega_c=20/0,2407[s]=83,09[s]$.
2. For $G_C(s)$ the time delay/time constant ratio is $D_C/T_C=2,1/7,51=0,28<1$, hence, the influence of the time constant prevails - $G_C(s)$ is a so-called „lag-dominant system" with integrator, therefore B-parabolas are to be chosen carefully. From one side, due to time delay it would be desirable to choose B-parabolas from Fig. 14, Fig. 15 or Fig. 16 with the lowest identification level $\omega_n/\omega_c=0,2$. However, the minima of $B_{0,2}$ parabolas in Fig. 14b (for $\beta=4$), Fig. 15b (for $\beta=8$) and Fig. 16b (for $\beta=12$) indicate the smallest achievable relative settling time $\tau_s=36,5$ (for $\beta=4$), $\tau_s=33$ (for $\beta=8$) and $\tau_s=34$ (for $\beta=12$), which do not satisfy the required value $\tau_s=20$.
3. Identified points $G_C(j0,35\omega_c)=12,7e^{-j122°}$ and $G_C(j0,5\omega_c)=8,10e^{-j129°}$ are located on the plant frequency response $G_C(j\omega)$ (solid line) in Fig. 17a, verifying correctness of the sine-wave type identification.
4. The first performance specification $(\eta_{max1};\tau_s)=(30\%;20)$ can be provided using the $B_{0,35}$ parabolas for $\beta=12$ (Fig. 16b) at the level $\omega_n/\omega_c=0,35$ and for parameters $(\phi_{M1};\omega_{n1})=$ $=(53°;0,35\omega_c)$ (Design No. 1), supplying the augmented open-loop phase margin $\phi'_{M1}=\phi_{M1}+(180°/\pi)\omega_{n1}D_C=53°+10,1°=63,1°$ into the controller design algorithm. The second performance specification $(\eta_{max2};\tau_s)=(20\%,20)$ is achievable using the $B_{0,5}$ parabolas in Fig. 16 for $\beta=12$ and $\omega_n/\omega_c=0,5$ and parametres $(\phi_{M2};\omega_{n2})=(62°;0,5\omega_c)$ (Design No. 2). To reject the influence of D_C, instead of $\phi_{M2}=62°$ the augmented open-loop phase margin $\phi'_{M2}=\phi_{M2}+(180°/\pi)\omega_{n2}D_C=62°+14,5°=76,5°$ was supplied into the PID controller design algorithm.
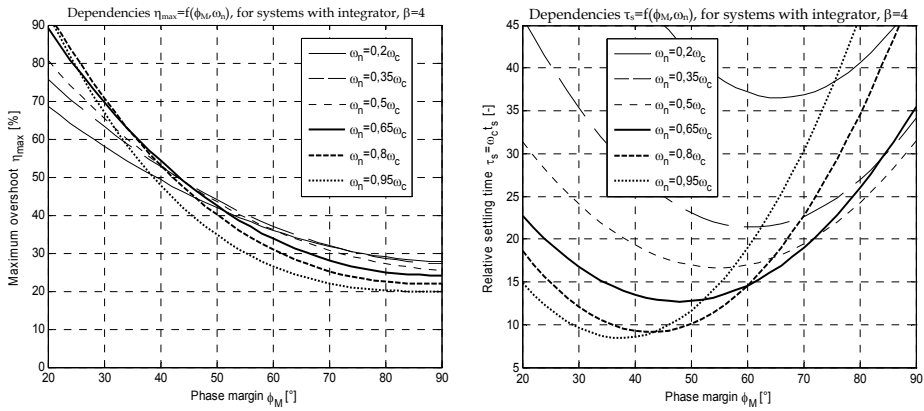
Fig. 14. B-parabolas: a) $\eta_{max}=f(\phi_M,\omega_n)$; b) $\tau_s=\omega_c t_s=f(\phi_M,\omega_n)$ for systems with integrator, $\beta=4$
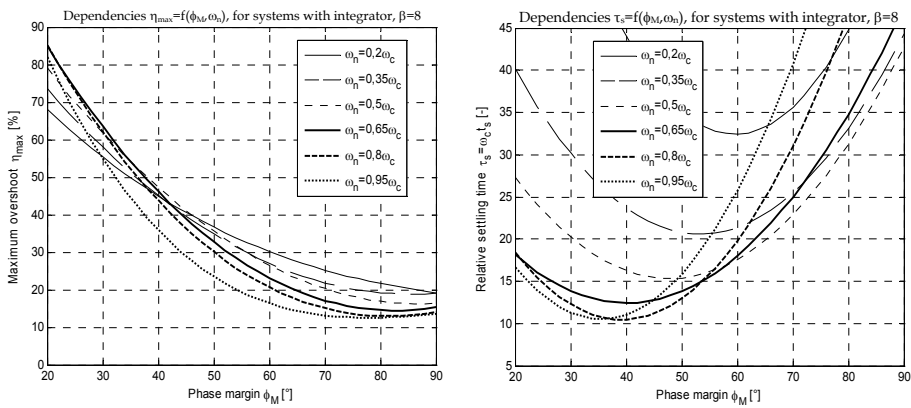

Fig. 15. B-parabolas: a) $\eta_{max}=f(\phi_M,\omega_n)$; b) $\tau_s=\omega_c t_s=f(\phi_M,\omega_n)$ for systems with integrator, $\beta=8$
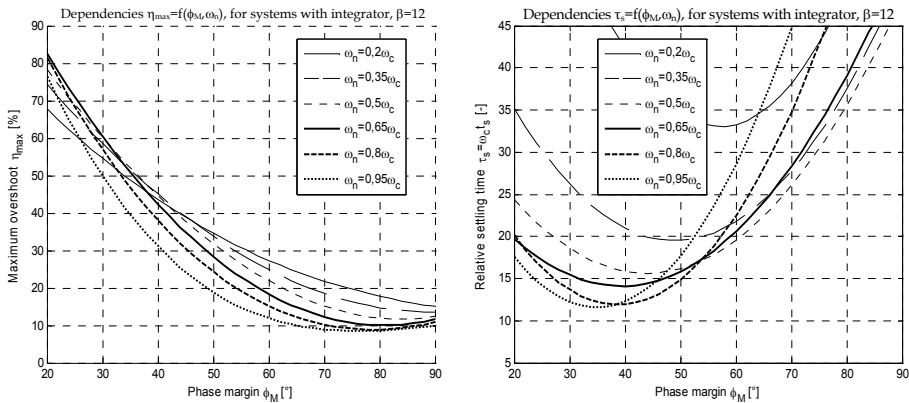

Fig. 16. B-parabolas: a) $\eta_{max}=f(\phi_M,\omega_n)$; b) $\tau_s=\omega_c t_s=f(\phi_M,\omega_n)$ for systems with integrator, $\beta=12$
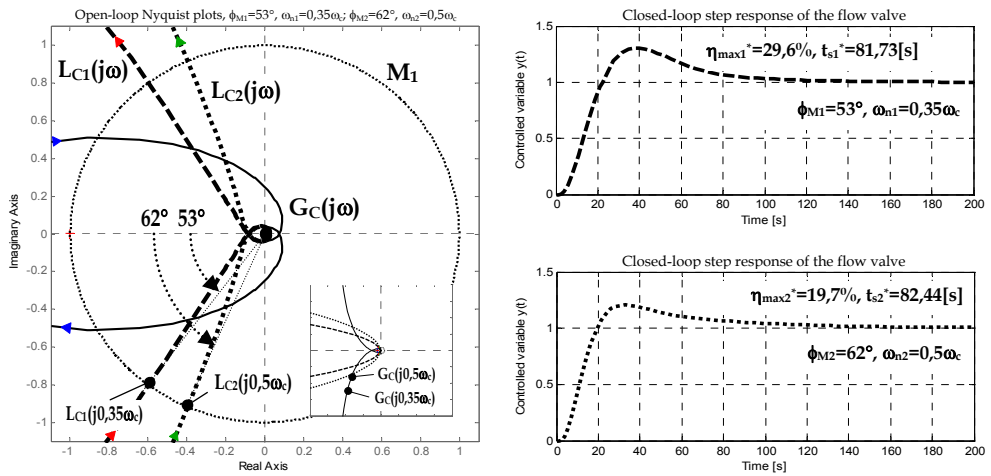
Fig. 17. a) Open-loop Nyquist plots; b) closed-loop step responses of the flow valve, required performance η_{max1}=30%, η_{max2}=20% and τ_s=20

5. Using the PID controller, the first identified point $G_C(j0,35\omega_c)$ (Design No. 1) was moved into the gain crossover $L_{C1}(j0,35\omega_c)=1e^{-j127^\circ}$ located on the unit circle M_1; this verifies achieving the phase margin $\phi_{M1}=180°-127°=53°$ (dashed line in Fig. 17a). Achieved performance in terms of the closed-loop step response in Fig. 17b is η_{max1}^*=29,6%, t_{s1}^*=81,73[s] (dashed line). The second identified point $G_C(j0,5\omega_c)$ (Design No. 2) was moved into $L_{C2}(j0,5\omega_c)=1e^{-j118^\circ}$ achieving the phase margin $\phi_{M2}=180°-118°=62°$ (dotted line in Fig. 17a). Achieved performance in terms of the closed-loop step response parameters η_{max2}^*=19,7%, t_{s2}^*=82,44[s] (dotted line in Fig. 17b) meets the required specification. Frequency characteristics $L_{C1}(j\omega)$, $L_{C2}(j\omega)$ begin near the negative real half-axis of the complex plane, because both open-loops contain a 2nd order integrator.

Discussion

All data necessary to design two PID controllers of all three plants $G_A(s)$, $G_B(s)$ and $G_C(s)$ along with specified and achieved performance measure values are summarized in Tab. 10 where η_{max} and t_s in the last two columns marked with „*" indicate closed-loop performance complying with the required one.

Model	η_{max};τ_s	ω_c[rad/s]	t_s[s]	B-par.	ϕ_M	ω_n/ω_c	$G(j\omega_n)$	$G_R(j\omega_n)$	η_{max}^*	t_s^*[s]
$G_A(s)$	30%;12	173,22	0,0693	Fig. 11	50°	0,5	$0,43e^{-j120^\circ}$	$2,31e^{-j10^\circ}$	29,7%	0,0584
$G_A(s)$	5%;12	173,22	0,0693	Fig. 11	70°	0,8	$0,19e^{-j165^\circ}$	$5,20e^{j55^\circ}$	4,89%	0,0605
$G_B(s)$	30%;12	0,3521	34,08	Fig. 11	55°+45,9°	0,35	$1,03e^{-j23^\circ}$	$0,97e^{-j56^\circ}$	18,6%	24,78
$G_B(s)$	5%;12	0,3521	34,08	Fig. 11	70°+26,2°	0,2	$1,09e^{-j13^\circ}$	$0,92e^{-j71^\circ}$	0,15%	28,69
$G_C(s)$	30%;20	0,2407	83,09	Fig. 16	53°+10,1°	0,35	$12,7e^{-j122^\circ}$	$0,08e^{j5,8^\circ}$	29,6%	81,73
$G_C(s)$	20%;20	0,2407	83,09	Fig. 16	62°+14,5°	0,5	$8,10e^{-j129^\circ}$	$0,12e^{-j28^\circ}$	19,7%	82,44

Table 10. Summary of required and achieved performance measure values, identification parametres and PID controller tunings for $G_A(s)$, $G_B(s)$ and $G_C(s)$

4. Conclusion

The proposed new engineering method based on the sine-wave identification of the plant provides successful PID controller tuning. The main contribution has been construction of empirical charts to transform engineering time-domain performance specifications (maximum overshoot and settling time) into frequency domain performance measures (phase margin). The method is applicable for shaping the closed-loop response of the process variable using various combinations of excitation signal frequencies and required phase margins. Using B-parabolas, it is possible to achieve optimal time responses of processes with various types of dynamics and improve their performance. When applying digital PID controller, it is recommended to set the sampling period T_s from the interval

$$T_s \in \left\langle \frac{0,2}{\omega_c}, \frac{0,6}{\omega_c} \right\rangle \qquad (46)$$

where ω_c is the critical frequency of the controlled plant (Wittenmark, 2001).

By applying appropriate PID controller design methods including the above presented 51+3 tuning rules for prescribed performance, it is possible to achieve cost-effective control of industrial processes. The presented advanced sine-wave design method offers one possible way to turn the unfavourable statistical ratio between properly tuned and all implemented PID controllers in industrial control loops.

5. Acknowledgment

6. References

Åström, K.J. & Hägglund, T. (1995). *PID Controllers: Theory, Design and Tuning* (2nd Edition), Instrument Society of America, Research Triangle Park, ISBN 1-55617-516-7

Åström, K.J. & Hägglund, T. (2000). Benchmark Systems for PID Control. *IFAC Workshop on Digital Control PID'00,* pp. 181-182, Terrassa, Spain, April, 2000

Bakošová, M. & Fikar, M. (2008). *Riadenie procesov (Process Control),* Slovak University of Technology in Bratislava, ISBN 978-80-227-2841-6, Slovak Republic (in Slovak)

Balátě, J. (2004). *Automatické řízení (Automatic Control)* (2nd Edition), BEN - technická literatúra, ISBN 80-7300-148-9, Praha, Czech Republic (in Czech)

Bucz, Š.; Marič, L.; Harsányi, L. & Veselý, V. (2010). A Simple Robust PID Controller Design Method Based on Sine Wave Identification of the Uncertain Plant. *Journal of Electrical Engineering,* Bratislava, Vol. 61, No. 3, (2010), pp. 164-170, ISSN 1335-3632

Bucz, Š.; Marič, L.; Harsányi, L. & Veselý, V. (2010). A Simple Tuning Method of PID Controllers with Prespecified Performance Requirements. *9th International Conference Control of Power Systems 2010,* High Tatras, Slovak Republic, May 18-20, 2010

Bucz, Š.; Marič, L.; Harsányi, L. & Veselý, V. (2010). Design-oriented Identification Based on Sine Wave Signal and its Advantages for Tuning of the Robust PID Controllers. *International Conference Cybernetics and Informatics,* Vyšná Boca, Slovak Republic, 2010

Bucz, Š.; Marič, L.; Harsányi, L. & Veselý, V. (2011). Easy Tuning of Robust PID Controllers Based on the Design-oriented Sine Wave Type Identification. *ICIC Express Letters,* Vol. 5, No. 3 (March 2011), pp. 563-572, ISSN 1881-803X, Kumamoto, Japan

Bucz, Š. (2011). *Engineering Methods of Robust PID Controller Tuning for Specified Performance.* Doctoral Thesis, Slovak University of Technology in Bratislava, Slovak Republic (in Slovak)

Coon, G.A. (1956). How to Find Controller Settings from Process Characteristics, In: *Control Engineering,* Vol. 3, No. 5, (May 1956), pp. 66-76

Chandrashekar, R.; Sree, R.P. & Chidambaram, M. (2002). Design of PI/PID Controllers for Unstable Systems with Time Delay by Synthesis Method, *Indian Chemical Engineer Section A,* Vol. 44, No. 2, pp. 82-88

Chau, P.C. (2002). Process Control - a First Course with MATLAB (1st edition), *Cambridge University Press,* ISBN 978-0521002554, New York

Chen, D. & Seborg, D.E. (2002). PI/PID Controller Design Based on Direct Synthesis and Disturbance Rejection, *Industrial Engineering Chemistry Research,* 41, pp. 4807-4822

Chien, K.L.; Hrones, J.A. & Reswick, J.B. (1952). On the Automatic Control of Generalised Passive Systems. *Transactions of the ASME,* Vol. 74, February, pp. 175-185

Ford, R.L. (1953). The Determination of the Optimum Process-controller Settings and their Confirmation by Means of an Electronic Simulator, *Proceedings of the IEE, Part 2,* Vol. 101, No. 80, pp. 141-155 and pp. 173-177, 1953

Grabbe, E.M.; Ramo, S. & Wooldrige, D.E. (1959-61). *Handbook of Automation Computation and Control,* Vol. 1,2,3, New York

Haalman, A. (1965). Adjusting Controllers for a Deadtime Process, *Control Engineering,* July

Hang, C.C. & Åström, K.J. (1988). Practical Aspects of PID Auto-tuners Based on Relay feedback, *Proceedings of the IFAC Adaptive Control of Chemical Processes Conference,* pp. 153-158, Copenhagen, Denmark, 1998

Harsányi, L.; Murgaš, J.; Rosinová, D. & Kozáková, A. (1998). *Teória automatického riadenia (Control Theory),* Slovak University of Technology in Bratislava, ISBN 80-227-1098-9, Slovak Republic (in Slovak)

Hudzovič, P. (1982). *Teória automatického riadenia I. Lineárne spojité systémy (Control theory: Linear Continuous-time Systems),* Slovak University of Technology in Bratislava, Slovak Republic (in Slovak)

Kozáková, A.; Veselý, V. & Osuský, J. (2010). Decentralized Digital PID Design for Performance. *In: 12th IFAC Symposium on Large Scale Systems: Theory and Applications,* Lille, France, 12.-14.7.2010, Ecole Centrale de Lille, ISBN 978-2-915-913-26-2

Morari, M., Zafiriou, E. (1989). *Robust Processs Control.* Prentice-Hall Inc., Englewood Cliffs, ISBN 0137821530, 07632 New Jersey, USA

O´Dwyer, A. (2006). *Handbook of PI and PID Controllers Tuning Rule* (2nd Edition), Imperial College Press, ISBN 1860946224, London

Osuský, J.; Veselý, V. & Kozáková, A. (2010). Robust Decentralized Controller Design with Performance Specification, *ICIC Express Letters,* Vol. 4, No. 1, (2010), pp. 71-76, ISSN 1881-803X, Kumamoto, Japan

Pettit, J.W. & Carr, D.M. (1987). Self-tuning Controller, *US Patent* No. 4669040

Rotach, V. (1984). Avtomatizacija nastrojki system upravlenija. *Energoatomizdat,* Moskva, Russia (in Russian)

Rotach, V. (1994). Calculation of the Robust Settings of Automatic Controllers, *Thermal Engineering (Russia),* Vol. 41, No. 10, pp. 764-769, Moskva, Russia

Suyama, K. (1992). A Simple Design Method for Sampled-data PID Control Systems with Adequate Step Responses, *Proceedings of the International Conference on Industrial Electronics, Control, Instrumentation and Automation,* pp. 1117-1122, 1992

Veselý, V. (2003). Easy Tuning of PID Controller. *Journal of Electrical Engineering,* Vol. 54, No. 5-6, (2003), pp. 136-139, ISSN 1335-3632, Bratislava, Slovak Republic

Visioli, A. (2001). Tuning of PID Controllers with Fuzzy Logic, *IEE Proceedings-Control Theory and Applications*, Vol. 148, No. 1, pp. 180-184, 2001

Visoli, A. (2006). *Practical PID Control, Advances in Industrial Control,* Springer-Verlag London Limited, ISBN 1-84628-585-2

Vítečková, M. (1998). *Seřízení regulátorů metodou požadovaného modelu (PID Controllers Tuning by Desired Model Method),* Textbook, VŠB – Technical University of Ostrava, ISBN 80-7078-628-0, Czech Republic (in Czech)

Vítečková, M. (1999). Seřízení číslicových i analogových regulátorů pro regulované soustavy s dopravním zpožděním (Tuning Discrete and Continuous Controllers for Processes with Time Delay). *Automatizace,* Vol. 42, No. 2, (1999), pp. 106-111, Czech Republic (in Czech)

Vítečková, M.; Víteček, A. & Smutný, L. (2000). Controller Tuning for Controlled Plants with Time Delay, *Preprints of Proceedings of PID'00: IFAC Workshop on Digital Control,* pp. 83-288, Terrassa, Spain, April 2000

Wang, L. & Cluett, W.R. (1997). Tuning PID Controllers for Integrating Processes, *IEE Proceedings - Control Theory and Applications,* Vol. 144, No. 5, pp. 385-392, 1997

Wang, Y.-G. & Shao, H.-H. (1999). PID Autotuner Based on Gain- and Phase-margin Specification, *Industrial Engineering Chemistry Research,* 38, pp. 3007-3012

Wittenmark, B. (2001). A Sample-induced Delays in Synchronous Multirate Systems, *European Control Conference*, Porto, Portugal, pp. 3276–3281, 2001

Wojsznis, W.K.; Blevins, T.L. & Thiele, D. (1999). Neural Network Assisted Control Loop Tuner, *Proceedings of the IEEE International Conference on Control Applications*, Vol. 1, pp. 427-431, USA, 1999

Xue, D.; Chen, Y. & Atherton, D.P. (2007). Linear Feedback Control. Analysis and Design with MATLAB, SIAM Press, ISBN 978-0-898716-38-2

Yu, Ch.-Ch. (2006). *Autotuning of PID Controllers. A Relay Feedback Approach* (2nd Edition), Springer-Verlag London Limited, ISBN 1-84628-036-2

Ziegler, J.G. & Nichols, N.B. (1942). Optimum Settings for Automatic Controllers, *ASME Transactions,* Vol. 64 (1942), pp. 759-768

Zhuang, M. & Atherton, D.P. (1993). Automatic Tuning of Optimum PID Controllers, *IEE Proceedings, Part D: Control Theory and Applications,* Vol. 140, No. 3, pp. 216-224, ISSN 0143-7054, 1993
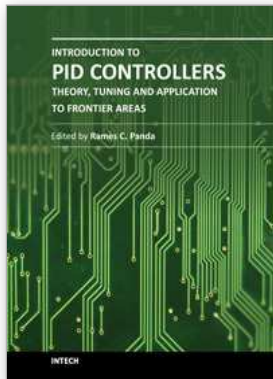
Introduction to PID Controllers - Theory, Tuning and Application to Frontier Areas

Edited by Prof. Rames C. Panda

This book discusses the theory, application, and practice of PID control technology. It is designed for engineers, researchers, students of process control, and industry professionals. It will also be of interest for those seeking an overview of the subject of green automation who need to procure single loop and multi-loop PID controllers and who aim for an exceptional, stable, and robust closed-loop performance through process automation. Process modeling, controller design, and analyses using conventional and heuristic schemes are explained through different applications here. The readers should have primary knowledge of transfer functions, poles, zeros, regulation concepts, and background. The following sections are covered: The Theory of PID Controllers and their Design Methods, Tuning Criteria, Multivariable Systems: Automatic Tuning and Adaptation, Intelligent PID Control, Discrete, Intelligent PID Controller, Fractional Order PID Controllers, Extended Applications of PID, and Practical Applications. A wide variety of researchers and engineers seeking methods of designing and analyzing controllers will create a heavy demand for this book: interdisciplinary researchers, real time process developers, control engineers, instrument technicians, and many more entities that are recognizing the value of shifting to PID controller procurement.

How to reference

In order to correctly reference this scholarly work, feel free to copy and paste the following:

INTECH
open science | open minds